Computational Studies on the Stabilities of *trans*-[Ir(OMe)(CO)(PPh_3)$_2$] and *trans*-[Ir(CH_2Me)(CO)(PPh_3)$_2$] toward β-H Elimination

Stuart A. Macgregor* and Prabha Vadivelu

School of Engineering and Physical Sciences, William Perkin Building, Heriot-Watt University, Edinburgh, EH14 4AS, U.K.

Received March 22, 2007

The relative stabilities of *trans*-[Ir(XMe)(CO)(PR_3)$_2$] species (X = O, CH_2) toward β-H elimination have been studied via combination of density functional and hybrid density functional/Hartree−Fock calculations. For both small (R = H) and full (R = Ph) model systems β-H elimination from the methoxide species is found to be disfavored both kinetically and thermodynamically compared to that from the analogous ethyl complexes. This is consistent with the greater stability of alkoxide species seen experimentally (R = Ph). In all cases the major contribution to the activation barrier is phosphine dissociation, and for the alkyl systems this leads directly to an agostically stabilized intermediate from which β-H transfer readily occurs. In contrast, with the *trans*-[Ir(OMe)(CO)(PR_3)$_2$] species a π-stabilized intermediate is formed and a further isomerization barrier must be overcome before β-H transfer can be accessed. Further calculations were performed on the acetophenone complex [Ir(H)(η^2-O=C(Me)Ph)(CO)(PPh_3)], and a low-energy pathway for face exchange of the metal-bound ketone has been characterized. This involves an η^1-intermediate and provides a mechanism for facile racemization of the precursor alkoxide. Selected calculations using alternative hybrid calculations showed the sensitivity of PPh_3 binding energies to the methodology employed. This is especially the case for the final step in the β-H elimination reaction, the formation of [Ir(H)(CO)(PPh_3)$_3$] from [Ir(H)(CO)(PPh_3)$_2$] and free PPh_3, where the use of the UFF approach appears to be particularly unreliable.

Introduction

The chemistry of low-valent transition metal alkoxides has gained impetus in recent years through the involvement of such species as intermediates in a number of important catalytic processes,[1] including aryl ether formation,[2] aldehyde/ketone hydrogenation,[3] and the aerobic oxidation of alcohols.[4] A characteristic reaction of metal alkoxides is β-H elimination to generate a metal hydride and free aldehyde or ketone. In each of the processes mentioned above control of β-H elimination is vital, either as a productive catalytic step[4] or as an undesirable decomposition route.[2,3]

β-H elimination from transition metal alkoxides most commonly occurs via a mechanism analogous to that established for transition metal alkyls, involving initial β-H transfer to an unsaturated metal center followed by elimination of the unsaturated organic.[5−7] The details of this process have been established for the decomposition of 16*e* [Pt(OMe)$_2$(dppe)] (dppe = 1,2-bis(diphenylphosphino)ethane), where reversible β-H transfer to Pt is followed by rate-limiting loss of methanol and formaldehyde.[8] A further well-characterized example is seen in iridium chemistry, where the formation of *mer-cis*-[Ir(Cl)(H)$_2$(PMe_3)$_3$] from *mer-cis*-[Ir(Cl)(H)(OMe)(PMe_3)$_3$] is promoted by the solvent-assisted dissociation of chloride, followed by irreversible β-H transfer and dissociative substitution of formaldehyde by chloride.[9] Most recently, Hartwig and coworkers have performed detailed mechanistic investigations of the β-H elimination reactions of *trans*-[Ir(OR)(CO)(PPh_3)$_2$] species,[10] first observed by Atwood and colleagues.[11] This work revealed that β-H elimination proceeds via initial reversible phosphine loss, reversible β-H transfer, and irreversible substitution of aldehyde/ketone by phosphine to yield, in the presence of added PPh_3, [Ir(H)(CO)(PPh_3)$_3$].

One intriguing aspect of low-valent metal alkoxides is their relative reactivity compared to analogous alkyls. In this light, *trans*-[Ir(OR)(CO)(PPh_3)$_2$] species display a marked stability, as β-H elimination requires temperatures in excess of 95 °C. This contrasts with the relative *instability* of an analogous alkyl, *trans*-[Ir(octyl)(CO)(PPh_3)$_2$], which undergoes very facile β-H elimination at 0 °C.[12] Only one other comparison

* Corresponding author. E-mail: s.a.macgregor@hw.ac.uk.

(1) For a review of low-valent transition metal alkoxide chemistry up to the late 1980s see: Bryndza, H. E.; Tam, W. *Chem. Rev.* **1988**, *88*, 1163.

(2) (a) Hartwig, J. F. *Synlett* **2006**, 1283. (b) Muci, A. R.; Buchwald, S. L. *Top. Curr. Chem.* **2002**, *219*, 131.

(3) (a) Clapham, S. E.; Hadzovic, A.; Morris, R. H. *Coord. Chem. Rev.* **2004**, *248*, 2201. (b) Noyori, R.; Yamakawa, M.; Hashiguchi, S. *J. Org. Chem.* **2001**, *66*, 7931.

(4) (a) Schultz, M. J.; Sigman, M. S. *Tetrahedron* **2006**, *62*, 8227. (b) Stahl, S. S. *Science* **2005**, *309*, 1824. (c) Stoltz, B. M. *Chem. Lett.* **2004**, *33*, 362.

(5) A variety of different mechanisms for the β-hydrogen elimination reactions of low-valent metal alkoxides have also been identified that would not necessarily be available for analogous alkyls. These include solvent-assisted methoxide dissociation followed by C−H bond activation[6] as well as a binuclear decomposition pathway.[7]

(6) Blum, O.; Milstein, D. *J. Organomet. Chem.* **2000**, *593*, 479.

(7) Ritter, J. C. M.; Bergman, R. G. *J. Am. Chem. Soc.* **1998**, *120*, 6826.

(8) Bryndza, H. E.; Calabrese, J. C.; Marsi, M.; Roe, C. D.; Tam. W.; Bercaw, J. E. *J. Am. Chem. Soc.* **1986**, *108*, 4805.

(9) Blum, O.; Milstein, D. *J. Am. Chem. Soc.* **1995**, *117*, 4582.

(10) Zhao, J.; Hesslink, H.; Hartwig, J. F. *J. Am. Chem. Soc.* **2001**, *123*, 7220.

(11) Bernard, K. A.; Rees, W. M.; Atwood, J. D. *Organometallics* **1986**, *5*, 390.

(12) (a) Schwartz, J.; Cannon, J. B. *J. Am. Chem. Soc.* **1974**, *96*, 2277. (b) Bergwall, C.; Parsons, E. J. *J. Organomet. Chem.* **1994**, *483*, 73.

10.1021/om700276p CCC: $37.00
Publication on Web 06/20/2007

of analogous late transition metal alkoxide and alkyl species is available; however, in that case the stability trend was reversed: [Pt(OMe)$_2$(dppe)] decomposes at 25 °C, while [Pt(CH$_2$Me)$_2$(dppe)] required temperatures in excess of 160 °C.[8] The mixed species [Pt(CH$_2$Me)(OMe)(dppe)] decomposes at an intermediate temperature (100 °C), and labeling studies suggest that β-H elimination from the ethyl ligand in this species is slightly more favorable kinetically than that from the alkoxide.

Experimental studies of β-H elimination have been complemented by a large body of computational work, and numerous studies on transition metal alkyls have appeared.[13] For transition metal alkoxides only a few studies have considered the complete β-H elimination process. These have shown the most difficult step can often be the formation of a vacant metal site prior to β-H transfer. Thus for [Ru(Cl)(OMe)(HOMe)(PH$_3$)$_3$] (methanol dissociation),[14] [Ru(OMe)(NH$_2$CH$_2$CH$_2$O)(η^6-C$_6$H$_6$)] ($\eta^6-\eta^4$ slippage),[15] and [Pd(OMe)(OH)(NH=CHCH=NH)] (chelate arm dissociation)[16] large barriers are involved for the ligand dissociation steps indicated. However, once a vacant site is available, β-H transfer is relatively facile.[17,18] Most recently a study of β-H elimination from [(−)(sparteine)PdCl(OCH$_2$Ph)] defined a barrier of 18.8 kcal/mol for β-H transfer; however this step was closely coupled to the concomitant displacement of the Cl ligand.[19] Similarly, high activation barriers for β-H transfer can be seen when this process is coupled to product release, as in the concerted β-H transfer/formaldehyde elimination computed from four-coordinate [M(OMe)(X)L$_2$] model species (M = Pd, Pt; L$_2$ = diimine or diphosphine chelating ligands).[16] An additional factor that may raise the barrier for β-H transfer is the ability of alkoxide ligands to stabilize unsaturated intermediates through π-donation. This effect has been seen in [Ir(OMe)(H)(PH$_3$)$_3$]$^+$ model species, where a barrier of over 12 kcal/mol for the β-H transfer step was computed.[20]

Despite the above work, there remain very few studies where the reactivity of analogous transition metal alkyls and alkoxides toward β-H elimination are directly compared.[21] We have therefore undertaken a computational study to account for the very different stabilities of the analogous *trans*-[Ir(OR)(CO)(PPh$_3$)$_2$] and *trans*-[Ir(CH$_2$R)(CO)(PPh$_3$)$_2$] species toward this process. The calculations will be based on the mechanism proposed by Hartwig and co-workers for β-H elimination from *trans*-[Ir(OR)(CO)(PPh$_3$)$_2$] species.[10] We shall show that the key difference that accounts for the greater stability of the *trans*-[Ir(OR)(CO)(PPh$_3$)$_2$] species lies in the ability of the alkoxide ligand to act as a stabilizing π-donor in the unsaturated metal intermediate involved. In addition, we also propose a low-energy mechanism that accounts for facile alkoxide ligand racemization in appropriate enantiopure *trans*-[Ir(OCHRR′)(CO)(PPh$_3$)$_2$] species.

Computational Details

All calculations were run with Gaussian 98.[22] For the small model systems, *trans*-[Ir(XMe)(CO)(PH$_3$)$_2$] (X = O, CH$_2$), full density functional theory (DFT) calculations employing the BP86 functional were used. Ir and P centers were described with the Stuttgart RECPs and associated basis sets[23] with a set of d-orbital polarization functions on P (ζ = 0.387).[24] 6-31G** basis sets were used for all other atoms.[25] All stationary points were fully characterized via analytical frequency calculations as either minima (all positive eigenvalues) or transition states (one imaginary eigenvalue), and IRC calculations were used to confirm the minima linked by each transition state. Energies include a correction for zero-point energies, and free energies are quoted at 298.15 K.

The large size of the full [Ir(XMe)(CO)(PPh$_3$)$_2$] systems (X = O, CH$_2$) meant that it was impractical to attempt geometry optimization at the full DFT level. Instead, hybrid approaches have been adopted using the ONIOM scheme. This requires the full molecule to be divided into layers that are then treated at different levels of theory. For the [Ir(XMe)(CO)(PPh$_3$)$_2$] systems this entailed the computation of the full molecule at a "low" level of theory. In addition a small model incorporating the reactive {Ir(XMe)(CO)(PH$_3$)$_2$} core was defined and computed at both a "high" and the "low" level of theory. For all the hybrid calculations in this study the high level of theory used the BP86 functional with the same ECP/basis set combinations used above for the PH$_3$ model calculations. Most of the hybrid results reported in the text are based on optimizations using Hartree−Fock theory for the low level (denoted BP86/HF). These employed lanl2dz pseudopotentials[26] and basis sets for Ir and P (retaining the d-orbital polarization on P) with all other atoms being described with 6-31G basis sets. Where possible, experimental data were used to provide initial geometries for optimization, and structures for both *trans*-[Ir(OMe)(CO)(PPh$_3$)$_2$] and *trans*-[Ir(CH$_2$Me)(CO)(PPh$_3$)$_2$] were adapted from the molecular structure of *trans*-[Ir(OPh)(CO)(PPh$_3$)$_2$].[27] Similarly, the structure of [Ir(H)(CO)(PPh$_3$)$_3$] was adapted from the published structure of the Rh analogue.[28] Other structures were derived from these species via the reaction profiles discussed in the text. The nature of all stationary points was then confirmed via analytical frequency calculations. As IRC calculations are not available for hybrid calculations, transition states were further characterized by displacing the geometry in such a way to mimic the unique imaginary frequency and then allowing these structures to relax to the adjacent local minima. The energies of all stationary points generated with the BP86/HF calculations were then recalculated with the BP86 functional, employing lanl2dz pseudopotentials and basis sets for Rh and P (plus polarization on P) and 6-31G** basis sets on C, O, and H. A zero-point energy correction derived from the BP86/HF calculations was applied to these BP86 SCF energies, and the final

(13) Niu, S.; Hall, M. B. *Chem. Rev.* **2000**, *100*, 353. (b) Dedieu, A. *Chem. Rev.* **2000**, *100*, 543.

(14) Itagaki, H.; Koga, N.; Morokuma, K.; Saito, Y. *Organometallics* **1993**, *12*, 1648.

(15) Yamakawa, M.; Ito, H.; Noyori, R. *J. Am. Chem. Soc.* **2000**, *122*, 1466.

(16) Ng, S. M.; Zhao, C.; Lin, Z. *J. Organomet. Chem.* **2002**, *662*, 120.

(17) See also studies where the energetics of β-H transfer have been defined: (a) Huo, C.-F.; Li, Y.-W.; Beller, M.; Jiao, H. *Organometallics* **2004**, *23*, 2168. (b) Versluis, L.; Ziegler, T. *J. Am. Chem. Soc.* **1990**, *112*, 6763.

(18) β-H transfer has also been studied for the bare [Fe(OMe)]$^+$ cation and entails a very high barrier of 37 kcal/mol. This was attributed to the high-spin state of the reactant (S = 5/2) and the consequent lack of vacant orbitals for interaction with the approaching C−H bond. Fiedler, A.; Schröder, D.; Schwarz, H.; Tjelta, B. L.; Armentrout, P. B. *J. Am. Chem. Soc.* **1996**, *118*, 5047.

(19) Nielsen, R. J.; Keith, J. M. Stoltz, B. M.; Goddard, W. A., III. *J. Am. Chem. Soc.* **2004**, *126*, 7967.

(20) Macgregor, S. A.; Sweeney, B. *New J. Chem.* **2000**, *24*, 851.

(21) Ziegler and co-workers have compared the β-H transfer step in [Co(XCH$_3$)(CO)$_3$] species (X = O,[17b] CH$_2$) and found each proceeded with similar small barriers of less than 2 kcal/mol. See: Versluis, L.; Ziegler, T.; Fan, L. *Inorg. Chem.* **1990**, *29*, 4530.

(22) Frisch, M.; et al. *Gaussian 98*, Revision A.11.4; Gaussian, Inc.: Pittsburgh, PA, 2001.

(23) Andrae, D.; Häusserman, U.; Dolg, M.; Stoll, H.; Preuss, H. *Theor. Chim. Acta* **1990**, *77*, 123.

(24) Höllwarth, A.; Böhme, M.; Dapprich, S.; Ehlers, A. W.; Gobbi, A.; Jonas, V.; Köhler, K. F.; Stegmann, R.; Veldkamp, A.; Frenking, G. *Chem. Phys. Lett.* **1993**, *208*, 237.

(25) (a) Hehre, W. J.; Ditchfield, R.; Pople, J. A. *J. Chem. Phys.* **1972**, *56*, 2257. (b) Hariharan, P. C.; Pople, J. A. *Theor. Chim. Acta* **1973**, *28*, 213.

(26) Hay, P. J.; Wadt, W. R. *J. Chem. Phys.* **1985**, *82*, 299.

(27) Rees, W. M.; Churchill, M. R.; Fettinger, J. C.; Atwood, J. D. *Organometallics* **1985**, *4*, 2179.

(28) La Placa, S. J.; Ibers, J. A. *Acta Crystallogr* **1965**, *18*, 511.

corrected values are referred to as BP86//BP86/HF in the text. Incorporation of general solvation via the polarized continuum model (PCM) approach[29] (THF, $\epsilon = 7.58$) showed such medium effects to be minimal. Finally, in addition to the BP86/HF optimizations we have also run a set of equivalent hybrid calculations where the low level used the Universal Force Field (UFF). These BP86/UFF energies include a correction for zero-point energies at the BP86/UFF level.

Results and Discussion

Small Models. (i) *trans*-[Ir(OMe)(CO)(PH$_3$)$_2$], 1′$_{OMe}$. The computed geometries and energies for the stationary points involved in β-H elimination from **1′$_{OMe}$** are given in Figure 1. **1′$_{OMe}$** exhibits the expected square-planar coordination geometry around Ir, and all metal−ligand bond distances are in good agreement with those determined crystallographically for the closely related structure *trans*-[Ir(OPh)(CO)(PPh$_3$)$_2$].[27] One discrepancy is seen in the orientation of the OMe ligand that lies in the metal coordination plane in **1′$_{OMe}$**, while in both *trans*-[Ir(OPh)(CO)(PPh$_3$)$_2$] and the BP86/HF-computed structure of *trans*-[Ir(OMe)(CO)(PPh$_3$)$_2$] (see below) the OR ligand adopts a more perpendicular orientation. This difference presumably reflects the minimal steric demands of the small PH$_3$ model ligands in **1′$_{OMe}$**. Phosphine dissociation from **1′$_{OMe}$** was modeled by systematically increasing one Ir−P distance, and this led directly to the 14*e* intermediate **2′$_{OMe}$** ($E = +23.5$ kcal/mol). During PH$_3$ loss the geometry of the {Ir(OMe)(CO)(PH$_3$)} moiety evolved smoothly into a distinctive Y-shape (O1−Ir−C1 = 142.1°, O1−Ir−P = 133.1°) and the computed profile indicated the absence of any significant activation barrier beyond that associated with breaking the Ir−PH$_3$ bond. The distorted metal coordination geometry in **2′$_{OMe}$** causes a hybridization of a vacant metal-based b_2-type orbital toward the alkoxide ligand. The alkoxide can then participate in O → Ir π-donation, which will be maximized with an upright orientation of the OMe ligand (see Scheme 1). A similar effect has also been computed in the electronically analogous d^6 [Ir(H)(OMe)(PH$_3$)$_3$]$^+$ model system.[20,30] This π-stabilization also accounts for the shortening of the Ir−O distance upon PH$_3$ loss, from 2.03 Å in **1′$_{OMe}$** to 1.92 Å in **2′$_{OMe}$**.

Scheme 1

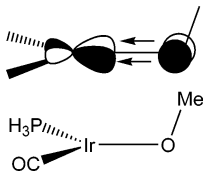

From **2′$_{OMe}$**, rotation about the Ir−O bond must occur to place a β-H *cis* to a vacant metal coordination site prior to β-H transfer. Depending on the direction of rotation, two intermediates may be formed where the β-H is either *trans* to PH$_3$ (T_{PH_3} **3a′$_{OMe}$**, $E = +24.8$ kcal/mol) or *trans* to CO (T_{CO} **3b′$_{OMe}$**, $E = +29.7$ kcal/mol). Both these species exhibit significant agostic interactions, the stronger being computed in the T_{PH_3} isomer (**3a′$_{OMe}$**: Ir···H1 = 1.83 Å, C1···H1 = 1.25 Å; **3b′$_{OMe}$**: Ir···H1 = 1.89 Å, C1···H1 = 1.23 Å). This reflects the lower *trans* influence of the PH$_3$ ligand in **3a′$_{OMe}$** and may contribute to the lower energy of this isomer, although favorable push−pull interactions[31] along the *trans*-OC−Ir−OMe axis in **3a′$_{OMe}$** will also play a role in this. For similar reasons, rotation about the Ir−O1 bond in **2′$_{OMe}$** to form T_{PH_3} **3a′$_{OMe}$** entails the lower barrier of 8.2 kcal/mol, 3 kcal/mol lower than the barrier to form T_{CO} **3b′$_{OMe}$**. This more accessible pathway involving the formation and subsequent reactivity of **3a′$_{OMe}$** is shown in Figure 1, and the subsequent discussion will focus on these lower energy processes.[32]

In **TS(2′-3a′)$_{OMe}$**, the transition state linking **2′$_{OMe}$** and **3a′$_{OMe}$**, the Ir−O1 bond is rotated by ca. 35° relative to **2′$_{OMe}$** and a distortion of the Ir coordination geometry toward a T_{PH_3} shape is also seen. Rotation is accompanied by an elongation of the Ir−O1 bond length, ultimately to 2.05 Å in **3a′$_{OMe}$**, and this reflects the less favorable O → Ir π-donation in the T_{PH_3} geometry. However, this is compensated by the gain of a strong agostic interaction, and so T_{PH_3} **3a′$_{OMe}$** is only 1.3 kcal/mol higher in energy than π-stabilized **2′$_{OMe}$**. From **3a′$_{OMe}$** β-H transfer readily occurs via **TS(3a′-4a′)$_{OMe}$** with a minimal activation barrier of 1 kcal/mol to give [Ir(H)(η^2-O=CH$_2$)(CO)(PH$_3$)] with H *trans* to PH$_3$ (**4a′$_{OMe}$**, $E = +23.0$ kcal/mol). The O=CH$_2$ ligand in **4a′$_{OMe}$** has an η^2-geometry; however unusually, the {CH$_2$} moiety is pushed well out of the coordination plane such that the x−Ir−C2 angle is only 145.8° (where x is the C1−O1 midpoint). We believe that this distorted geometry arises from enhanced π-back-donation from the Ir d_{z^2}-orbital into the O=CH$_2$ π*-acceptor orbital. The fact that it is the {CH$_2$} group that moves out of the plane reflects the larger p-orbital contribution to the π*-orbital on that center (see Scheme 2).[33] A similar explanation has been put forward to account for the distorted structure of *trans*-[Rh{PCyp$_2$(*c*-C$_5$H$_7$)}$_2$]$^+$, where dehydrogenation of one cyclopentyl substituent on each phosphine leads to a bis-phosphine, bis-alkene geometry with a narrow x−Rh−x angle of 149.0°.[34] Interestingly, this type of distortion seems to require a *trans* arrangement of π-acceptor ligands, as both *cis*-[Rh{PCyp$_2$(*c*-C$_5$H$_7$)}$_2$]$^+$ and **4b′$_{OMe}$**, the isomer of **4a′$_{OMe}$** with O=CH$_2$ *cis* to CO, exhibit planar geometries.

Scheme 2

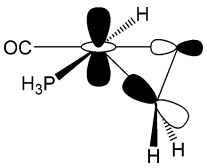

From **4a′$_{OMe}$**, the β-H elimination process continues via an associative displacement of O=CH$_2$ by PH$_3$. We found PH$_3$ addition to **4a′$_{OMe}$** to be a barrierless process, which produces five-coordinate [Ir(H)(η^2-O=CH$_2$)(CO)(PH$_3$)$_2$] (**5′$_{OMe}$**, $E = +2.3$ kcal/mol) with a trigonal bipyramidal geometry and axial H and PH$_3$ ligands. Formaldehyde dissociation from **5′$_{OMe}$** requires 15.9 kcal/mol and leads directly to *cis*-[Ir(H)(CO)(PH$_3$)$_2$] (***cis*-6′**, $E = +18.2$ kcal/mol). In the final step ***cis*-6′** is trapped via a further barrierless PH$_3$ addition to give five-coordinate [Ir(H)(CO)(PH$_3$)$_3$] (**7a′**, $E = +3.2$ kcal/mol) with two equatorial

(29) Cancès, M. T.; Mennucci, B.; Tomasi, J. *J. Chem. Phys.* **1997**, *107*, 3032.

(30) Riehl, J.-F.; Jean, Y.; Eisenstein, O.; Pélissier, M. *Organometallics* **1992**, *11*, 729.

(31) Caulton, K. G. *New J. Chem.* **1994**, *18*, 25.

(32) β-H transfer in **3b′$_{OMe}$** also involves a higher activation energy (+3.4 kcal/mol) than that associated with the T_{PH_3} form, and this again reflects the greater *trans* influence of CO compared to PH$_3$. Full details of the formation and reactivity of T_{CO} **3b′$_{OMe}$** are given as Supporting Information.

(33) The computed energy of the form with X−Ir−C2 = 145.8° but now with the oxygen of the η^2-O=CH$_2$ ligand moved out of the metal coordination plane is 23 kcal/mol higher in energy.

(34) Weller, A. S.; Brayshaw, S. K.; Douglas, T. M.; Moxham, G. L.; Macgregor, S. A.; Vadivelu, P.; Wondimagegn, T. Manuscript in preparation.

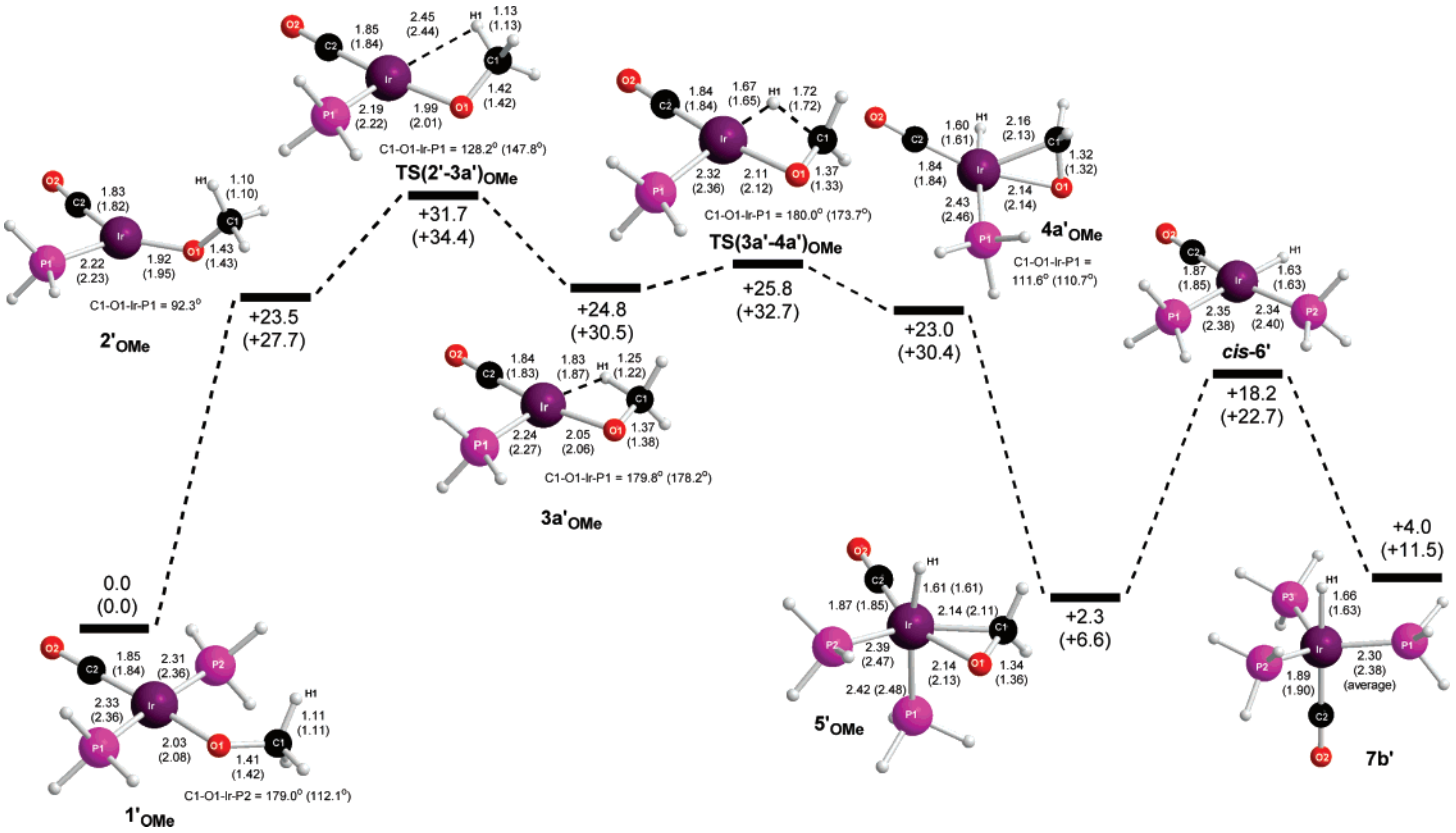

Figure 1. Computed reaction profile (kcal/mol) for β-H elimination from *trans*-[Ir(OMe)(CO)(PH_3)$_2$], where H is transferred *trans* to PH_3. Selected distances are given in Å, and equivalent data for *trans*-[Ir(OMe)(CO)(PPh_3)$_2$] are shown in parentheses.

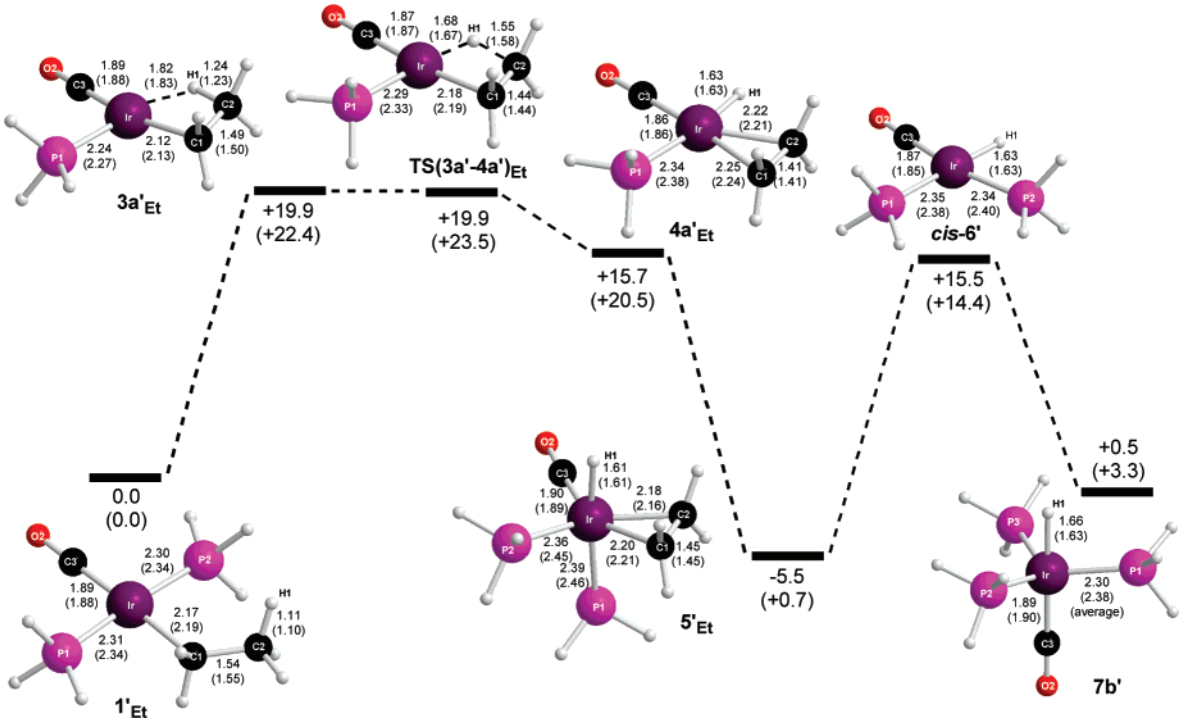

Figure 2. Computed reaction profile (kcal/mol) for β-H elimination from *trans*-[Ir(CH$_2$Me)(CO)(PH$_3$)$_2$], where H is transferred *trans* to PH$_3$. Selected distances are given in Å, and equivalent data for *trans*-[Ir(CH$_2$Me)(CO)(PPh$_3$)$_2$] are shown in parentheses.

phosphine ligands. Experimentally, [Ir(H)(CO)(PPh$_3$)$_3$] is thought to have all three PPh$_3$ ligands in equatorial positions,[35] and we compute this latter form, **7b′**, to be 0.8 kcal/mol higher in energy than **7a′**. This discrepancy again reflects the small steric bulk of the PH$_3$ model ligands, as the relative energies of **7a** and **7b** swap when the full [Ir(H)(CO)(PPh$_3$)$_3$] molecule is computed (see below). Figure 1 gives the structure and energies of the experimentally relevant all-equatorial isomer, **7b′**.

(ii) *trans*-[Ir(CH$_2$Me)(CO)(PH$_3$)$_2$], 1′$_{Et}$. In contrast to its OMe analogue, PH$_3$ dissociation from **1′$_{Et}$** leads directly to an agostic complex, T$_{PH_3}$ **3a′$_{Et}$** (see Figure 2). The geometry of **3a′$_{Et}$**, with Ir···H1 = 1.82 Å and C1···H1 = 1.24 Å, suggests a degree of agostic interaction similar to that computed in **3a′$_{OMe}$**. **3a′$_{Et}$** is however relatively more accessible, being only 19.9 kcal/mol higher in energy than **1′$_{Et}$**, whereas **3a′$_{OMe}$** is 24.8 kcal/mol higher than **1′$_{OMe}$**. β-H transfer from **3a′$_{Et}$** occurs with a minimal barrier to give [Ir(H)(C$_2$H$_4$)(CO)(PH$_3$)] (**4a′$_{Et}$**, E = +15.7 kcal/mol) with H *trans* to PH$_3$. PH$_3$ addition to **4a′$_{Et}$** is a barrierless process and gives [Ir(H)(C$_2$H$_4$)(CO)(PH$_3$)$_2$] (**5′$_{Et}$**, E = −5.5 kcal/mol). β-H elimination is then completed by alkene dissociation to give ***cis*-6′**, which is then trapped by added PH$_3$ to produce **7a′**. These final two processes are identical to those characterized along the β-H elimination pathway of **1′$_{OMe}$**, and Figure 2 again shows details of the all-equatorial isomer of the product, **7b′**.[36]

Comparison of the reaction profiles in Figures 1 and 2 indicates that the key step determining the ease of β-H elimination from **1′$_{OMe}$** and **1′$_{Et}$** involves the formation of the T$_{PH_3}$ β-agostic intermediates, **3a′**. Once these intermediates are formed, β-H transfer is an extremely facile process and the subsequent elimination of the unsaturated organic ligand occurs with similar barriers in each case. The two systems differ, however, in the ease of formation of T$_{PH_3}$ **3a′**. For **1′$_{OMe}$** this involves the initial formation of the π-stabilized species **2′$_{OMe}$**, which must then undergo a further isomerization via Ir−O bond rotation. These processes entail a combined activation barrier of 31.7 kcal/mol. For **1′$_{Et}$** PH$_3$ dissociation leads directly to T$_{PH_3}$ **3a′$_{Et}$**, and this requires only 19.9 kcal/mol. β-H transfer then occurs without any significant additional barrier. The overall energy change associated with β-H elimination to form **7b′** is also slightly more favorable for **1′$_{Et}$**, this being +0.5 kcal/mol compared to +4.0 kcal/mol for **1′$_{OMe}$**. The calculations on these small model systems are therefore consistent with the observation that β-H elimination from Ir-alkyls such as *trans*-[Ir(C$_8$H$_{17}$)(CO)(PPh$_3$)$_2$] readily occurs at 0 °C, whereas higher temperatures in excess of 95 °C are required for the equivalent process in analogous Ir-alkoxides such as *trans*-[Ir(OMe)(CO)(PPh$_3$)$_2$]. The calculations indicate that this difference is linked to the relatively high energy barrier associated with the formation and isomerization of the π-stabilized intermediate, **2′$_{OMe}$**.[37]

Full Model Systems. As described in the Computational Details, we have employed hybrid calculations to take account of the steric and electronic effects of the full PPh$_3$ ligands on the β-H elimination reactions of **1$_{OMe}$** and **1$_{Et}$**. The results are included in parentheses in Figures 1 and 2 and are based on BP86//BP86/HF calculations, i.e., full DFT BP86 single-point energies based on the hybrid BP86/HF-optimized geometries. The key features of the β-H elimination reaction profiles from **1$_{OMe}$** and **1$_{Et}$** are similar to those found with PH$_3$ model systems, and in the following we shall consider only the lower energy

(35) Bath, S. S.; Vaska, L. *J. Am. Chem. Soc.* **1963**, *85*, 3500.

(36) In principle, isomerization of T$_{PH_3}$ **3a′$_{Et}$** to T$_{CO}$ **3b′$_{Et}$** could occur, and a transition state for this process was located with a Y$_{Et}$ geometry very similar to **2$_{OMe}$**. In this case, however, the inability of the Et ligand to act as a π-donor results in a very high energy (+39.8 kcal/mol) and hence a very high barrier to isomerization. Moreover, subsequent β-H transfer in **3b′$_{Et}$** also has a larger barrier than that in **3a′$_{Et}$**, and so β-H elimination via **3a′$_{Et}$** will be favored on both counts. Full details of the formation and reactivity of **3b′$_{Et}$** are given in the Supporting Information.

(37) The inclusion of entropy has a similar effect on the activation barrier for both systems, as the rate-determining step in each case involves PH$_3$ dissociation. The free energies of activation are therefore lowered by about 10 kcal/mol, to +21.7 kcal/mol for **1′$_{OMe}$** and to +9.8 kcal/mol for **1′$_{Et}$**. The overall free energies of β-H elimination are less affected, and the reaction of **1′$_{Et}$** (ΔG = +0.6 kcal/mol) is still slightly thermodynamically favored over that of **1′$_{OMe}$** (ΔG = +2.7 kcal/mol).

Scheme 3

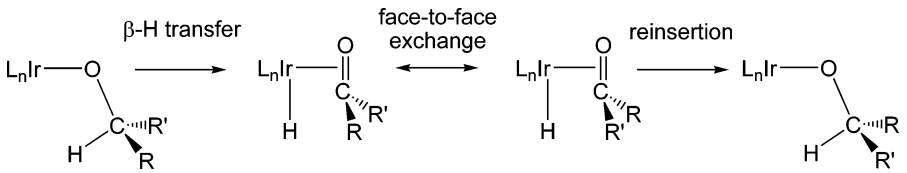

pathways involving β-H transfer *trans* to phosphine. The BP86/HF-computed geometries with the PPh_3 models are relatively unchanged compared to the smaller model analogues, with the most general effect being an elongation of the Ir−P distances, especially in the five-coordinate structures, where steric congestion is greatest.

(i) *trans*-[Ir(OMe)(CO)(PPh_3)$_2$], $\mathbf{1_{OMe}}$. Figure 1 shows that, while the β-H elimination reaction proceeds in a similar way to that found for $\mathbf{1'_{OMe}}$, there is a general increase in the energy of all the stationary points located after the initial PPh_3 dissociation. As before, the combined barrier for PPh_3 loss from $\mathbf{1_{OMe}}$ and the Ir−O rotation step in $\mathbf{2_{OMe}}$ to form $\mathbf{3a_{OMe}}$ represents the overall activation energy for β-H elimination. This has a value of +34.4 kcal/mol in this case, 2.7 kcal/mol higher than was computed for $\mathbf{1'_{OMe}}$. The major factor in this increase is the higher PPh_3 dissociation energy in $\mathbf{1_{OMe}}$ (27.7 kcal/mol) compared to PH_3 loss in $\mathbf{1'_{OMe}}$ (23.5 kcal/mol).

The inclusion of PPh_3 ligands has only a minor effect on the β-H transfer step in $\mathbf{3a_{OMe}}$, with the activation barrier increasing slightly from 1.0 kcal/mol to 2.2 kcal/mol. $\mathbf{4a_{OMe}}$ exhibits the same distorted geometry as seen before in the small model with an x−Ir−C2 angle of 143.0°. The β-H elimination process is completed by addition of PPh_3 to form via five-coordinate $\mathbf{5_{OMe}}$, from which O=CH_2 dissociates to give ***cis*-6**. Reaction profiles showed that neither step involved a transition state. A further barrierless PPh_3 addition step led to the formation of [Ir(H)(CO)(PPh_3)$_3$], initially as **7a**, the isomer with axial PPh_3 and H ligands. However, unlike the small PH_3 model systems, at the BP86//BP86/HF level the experimentally observed isomer, **7b**, with axial H and CO ligands, is now the more stable form by 6.4 kcal/mol, and we assume that isomerization between the initially formed **7a** and the final product **7b** will be a facile process. Along the reaction profile it is the energy of this final product, **7b**, that is most affected by the change to the larger model system, and this is perhaps not surprising, as this is the only species with three bulky PPh_3 ligands. This effect means that the overall energy change associated with β-H elimination from $\mathbf{1_{OMe}}$ is +11.5 kcal/mol, somewhat less favorable than was found for the reaction of $\mathbf{1'_{OMe}}$, (+4.0 kcal/mol).

(ii) *trans*-[Ir(CH_2Me)(CO)(PPh_3)$_2$], $\mathbf{1_{Et}}$. The computed BP86//BP86/HF β-H elimination reaction profile from $\mathbf{1_{Et}}$ in Figure 2 again follows the same basic pathway as that determined for the small model system $\mathbf{1'_{Et}}$. The initial PPh_3 dissociation from $\mathbf{1_{Et}}$ to form $\mathbf{3a_{Et}}$ is again slightly harder in the larger model, and this, coupled with the subsequent β-H transfer to form $\mathbf{4a_{Et}}$, contributes to an activation barrier for β-H elimination of +23.5 kcal/mol, 3.6 kcal/mol higher than for $\mathbf{1'_{Et}}$. The relative destabilization of the five-coordinate product **7b** mentioned above means that β-H elimination from $\mathbf{1_{Et}}$ is slightly more endothermic at the BP86//BP86/HF level (ΔE = +3.3 kcal/mol).

Comparing the energetics for both β-H elimination processes at the BP86//BP86/HF level shows that the reaction of $\mathbf{1_{Et}}$ is again significantly favored kinetically ($\Delta E^{\ddagger}$ = +23.5 kcal/mol, cf. +34.4 kcal/mol for $\mathbf{1_{OMe}}$) and thermodynamically (ΔE = +3.3 kcal/mol, cf. +11.5 kcal/mol). Interestingly, the difference in activation energy between $\mathbf{1_{Et}}$ and $\mathbf{1_{OMe}}$ is fairly constant in the two *trans*-[Ir(XCH_3)(CO)(PR_3)$_2$] model systems employed (R = H, $\Delta\Delta E^{\ddagger}$ = 11.8 kcal/mol; R = Ph, $\Delta\Delta E^{\ddagger}$ = 10.9 kcal/mol). The overall energy change is, however, somewhat more model dependent (R = H, $\Delta\Delta E$ = 2.7 kcal/mol; R = Ph, 8.2 kcal/mol), and this point will be discussed further below.

Mechanism of Inversion of Chiral Alkoxides. In the experimental study of β-H elimination, enantiopure *trans*-[Ir(OCH(R)R′)(CO)(PPh_3)$_2$] species bearing chiral alkoxides were found to undergo racemization at rates that depended on the concentration of added phosphine.[10] This observation established that release of ketone proceeds via associative displacement by phosphine. Inversion of configuration at the alkoxide carbon can be explained by a face-to-face rearrangement of the ketone intermediate formed upon β-H transfer and reinsertion into the Ir−H bond (see Scheme 3). At low phosphine concentration this process must be competitive with irreversible ketone loss. In addition, crossover experiments showed that racemization occurs without dissociation of the ketone from the metal coordination sphere. The details of the face-to-face exchange mechanism are not known, however, and so we have investigated this process computationally using both the small model species [Ir(H)(O=CH_2)(CO)(PH_3)], $\mathbf{4a'_{OMe}}$, and the acetophenone complex, [Ir(H)(O=C(Me)Ph)(CO)(PPh_3)], **8a**, derived from the chiral alkoxide, *trans*-[Ir(OCH(Me)Ph)(CO)(PPh_3)$_2$].

With η^2-$\mathbf{4a'_{OMe}}$ we found that elongation of the Ir−C1 bond led to the formation of an η^1-bound isomer with an activation barrier via $\mathbf{TS(\eta^2/\eta^1\text{-}4a')_{OMe}}$ of 8.1 kcal/mol (see Figure 3) η^1-$\mathbf{4a'_{OMe}}$ is 5.9 kcal/mol less stable than the η^2-form and features an in-plane orientation of the O=CH_2 ligand. Shortening the Ir−C1 distance such that C1 moves below the coordination plane generates a second transition state equivalent to $\mathbf{TS(\eta^2/\eta^1\text{-}4a')_{OMe}}$ and completes the face-to-face exchange process.

The most stable form of the η^2-acetophenone complex [Ir(H)(η^2-O=C(Me)Ph)(CO)(PPh_3)], η^2-**8a**, was located when the phenyl substituent is *trans* with respect to the PPh_3 ligand, and presumably this is favored for steric reasons. Elongation of the Ir−C1 bond again resulted in $\eta^2-\eta^1$ isomerization; however, in this case the ketone in the η^1-isomer lies approximately perpendicular to the metal coordination plane (η^1-**8a**, E = −4.9 kcal/mol, C1−O1−Ir−P1 = 116.2°). η^1-**8a** is formed via **TS(η^2/η^1-8a)** with a small activation barrier of only 3.0 kcal/mol and is located as the sterically less hindered *E*-isomer. In principle face-to-face exchange could be completed by re-forming η^2-**8a** such that the phenyl of the acetophenone is placed *cis* to the PPh_3 ligand. However, reaction profiles based on this process led to very high energies and no transition state could be located.[38] Instead an alternative low-energy pathway was characterized in which rotation about the Ir−O1 bond leads to the interconversion of two enantiomeric forms of η^1-**8a**. This process occurs with a barrier of only 1.2 kcal/mol, and in the transition state, **TS(η^1/η^1-8a)**, the acetopheneone ligand is virtually parallel to the metal coordination plane. The face-to-face exchange process is then completed by an $\eta^1-\eta^2$ isomerization that passes through a mirror-image form of **TS(η^2/η^1-8a)**.

(38) Attempts to compute this alternative η^2-form showed that this species did not correspond to a local minimum, as all geometries converged on the more stable η^1-isomer.

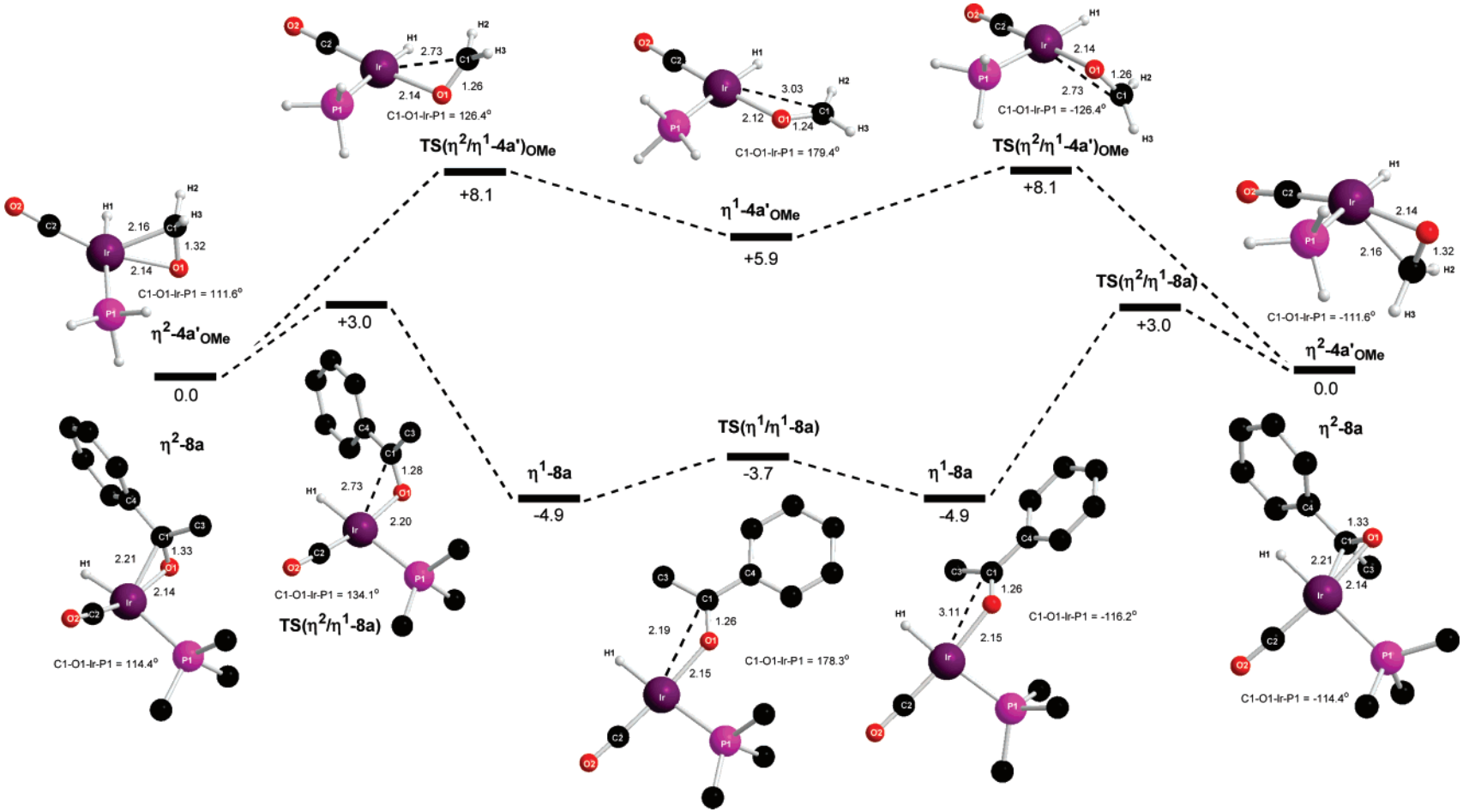

Figure 3. Computed reaction profiles (kcal/mol) for face-to-face exchange in [Ir(O═CH_2)(CO)(PH_3)] (**4a′$_{OMe}$**) and [Ir(C(Me)(Ph)O)(CO)(PPh_3)] (**8a**) with selected distances in Å. Acetophenone hydrogens are also omitted for clarity, while for space reasons only one form of η^1**-8a** and **TS(**η^2/η^1**-8a)** is shown. The omitted structures are mirror images of those drawn.

Comparing the reaction profiles in Figure 3 reveals important differences between the two systems. **4a′$_{OMe}$** is significantly more stable as the η^2-isomer, and $\eta^1-\eta^2$ isomerization entails a barrier of 8.1 kcal/mol. In contrast, **8a** is most stable in an η^1-geometry, and isomerization from the η^2-isomer involves a lower barrier of only 3.0 kcal/mol. Face-to-face exchange should therefore be reasonably accessible in species such as **η^2-8a**, and assuming facile reinsertion into the Ir−H bond in this species (cf. Scheme 3), this is consistent with the observation of racemization of the alkoxide (*R*)-*trans*-[Ir(OCH(Me)Ph)(CO)(PPh$_3$)$_2$].[10]

Transition metal complexes of η^1- and η^2-aldehydes and ketones are well known,[39] and examples of both structural types have been crystallographically characterized for formaldehyde[40,41] and acetophenone.[39,42] In general, η^2-geometries are seen when π-back-donation is favored, and this can be promoted by appropriately shaped metal fragments, highly electron-rich metal centers, and electron-withdrawing substituents on the O═CR$_2$ ligand.[43] Steric factors can also be important in controlling the coordination mode, and increased steric bulk will tend to favor η^1-geometries. On occasion the subtle balance of all these factors has led to the observation of equilibrium mixtures of both the η^1- and η^2-forms in solution.[44] For the {Ir(H)(CO)(PR$_3$)} fragments studied here it seems that there is an intrinsic preference for η^2-O═CH$_2$, while acetophenone always prefers the η^1-binding mode: computation of the complementary model systems [Ir(H)(O═CH$_2$)(CO)(PPh$_3$)] and [Ir(H)(O═C(Me)Ph)(CO)(PH$_3$)] shows that these preferences are maintained independent of the steric bulk of the phosphine.

Phosphine Binding Energies in *trans*-[Ir(XMe)(CO)(PPh$_3$)$_2$] and Related Species. To this point we have focused on our highest quality results obtained at the BP86//BP86/HF level. However, in the course of our study we also performed calculations with the BP86/UFF hybrid method. We therefore have the opportunity to compare three different approaches to computing these large PPh$_3$-containing systems, namely, BP86//BP86/HF, BP86/HF, and BP86/UFF. The basic finding that β-H elimination is kinetically more accessible for **1$_{Et}$** than **1$_{OMe}$** is maintained at all three levels of calculation, although the size of $\Delta\Delta E^{\ddagger}$ does show some variation, from 10 kcal/mol with BP86/HF to 14 kcal/mol with BP86/UFF. More marked, however, are differences in the various PPh$_3$ ligand binding energies when computed with the different methodologies, and we wish to comment on these here.

Table 1. Computed PR$_3$ Binding Energies (kcal/mol) in *trans*-[Ir(XMe)(CO)(PR$_3$)$_2$] (X = O, CH$_2$; R = H, Ph) and Related Systems

	R = Ph			R = H
	BP86/UFF	BP86/HF	BP86//BP86/HF	BP86
1$_{OMe}$ → 2$_{OMe}$	+32.7	+27.9	+27.7	+23.5
1$_{OMe}$ → 3a$_{OMe}$	+34.6	+29.7	+30.5	+24.8
1$_{Et}$ → 3a$_{Et}$	+30.0	+19.9	+22.4	+19.9
4a$_{OMe}$ → 5a$_{OMe}$	−28.6	−24.0	−23.8	−20.7
4a$_{Et}$ → 5a$_{Et}$	−25.1	−16.9	−19.8	−21.2
***cis*-6 → 7b**	−25.8	−6.0	−11.1	−14.2

The key PPh$_3$ ligand binding energies are summarized in Table 1 and show that these are always largest at the BP86/UFF level, while the BP86/HF and BP86//BP86/HF energies are generally quite close to each other. PPh$_3$ dissociation from **1$_{OMe}$** to form either **2$_{OMe}$** or **3a$_{OMe}$** is approximately 5 kcal/mol higher at the BP86/UFF level, whereas the difference increases to around 9 kcal/mol for PPh$_3$ loss from **1$_{Et}$** to form **3a$_{Et}$**. Similar trends are seen when PPh$_3$ is added to **4a**; the binding energy is again always higher at the BP86/UFF level, but the difference is larger for **4a$_{Et}$** than for **4a$_{OMe}$**. It is difficult to assess which method gives the "correct" answer in the absence of experimental data for comparison. However, we suspect that these subtle changes arise from the different treatment of interligand interactions and that this is responsible for the BP86/UFF approach producing intrinsically higher PPh$_3$ bonding energies. The fact that the difference between BP86/UFF and the other methods is smaller for **1$_{OMe}$** and **5$_{OMe}$** may be due to the presence of short O···H−C(*ortho*) contacts involving the PPh$_3$ ligands in these species that may contribute extra stabilization when treated with orbital methods.

The most extreme method dependency is, however, reserved for the addition of PPh$_3$ to ***cis*-6** to form **7b**, where the BP86/UFF approach gives an extremely high binding energy of 25.8 kcal/mol. This seems unrealistic given that the equivalent binding energy of PH$_3$ to ***cis*-6′** is only 14.2 kcal/mol and that the increased steric encumbrance in the tris-PPh$_3$ system formed might be expected to result in a lower binding energy. In addition, it has long been known that [Ir(H)(CO)(PPh$_3$)$_3$] readily undergoes PPh$_3$ ligand dissociation in solution to produce [Ir(H)(CO)(PPh$_3$)$_2$], which can then exhibit a range of reactivities.[45] This behavior would appear inconsistent with a high phosphine binding energy of over 25 kcal/mol. In contrast, the binding energies of PPh$_3$ to ***cis*-6** at both the BP86/HF and BP86//BP86/HF levels (6.0 and 11.1 kcal/mol, respectively) are lower than that of PH$_3$ to ***cis*-6′**, and absolute values of PPh$_3$ binding are more consistent with facile PPh$_3$ dissociation in **7b**. A possible reason for the high PPh$_3$ binding energy in **7b** is seen in the structure computed with the BP86/UFF approach, which displays a highly congested geometry with a number of short *ortho*-C−H···Ph contacts. Upon reoptimization at the BP86/HF level the structure of **7b** relaxes to a far more open form.

Overall it appears that PPh$_3$ binding energies are particularly sensitive to the methodology employed, and these are seriously overestimated with the BP86/UFF approach. The results presented here, along with other work in our group, suggest that this methodology overestimates interligand interactions, especially between triarylphosphine ligands.[46] For this reason the

(39) Helberg, L. E.; Gunnoe, T. B.; Brooks, B. C.; Sabat, M.; Harman, W. D. *Organometallics* **1999**, *18*, 573, and references therein.

(40) η^1-Formaldehyde: W. Saak, W.; Pohl, S. *Z. Anorg. Allg. Chem.* **1987**, *552*, 186.

(41) η^2-Formaldehyde: (a) Brown, K. L.; Clark, G. R.; Headford, C. E. L.; Marsden, K.; Roper, W. R. *J. Am. Chem. Soc.* **1982**, *104*, 2019. (b) Berke, H.; Huttner, G.; Weiler, G.; Zsolnai. *J. Organomet. Chem.* **1981**, *219*, 353. (c) Gambarotta, S.; Floriani, C.; Chiesivilla, A.; Guastini, C. *J. Am. Chem. Soc.* **1982**, *104*, 2019. (d) Gambarotta, S.; Floriani, C.; Chiesivilla, A.; Guastini C. *J. Am. Chem. Soc.* **1985**, *107*, 2985. (e) Rabinovich, D.; Parkin, G. *Inorg. Chem.* **1995**, *34*, 6341. (f) Hascall, T.; Murphy, V. J.; Janak, K. E.; Parkin, G. *J. Organomet. Chem.* **2002**, *652*, 37.

(42) η^1-Acetophenone: (a) Hevia, E.; Perez, J.; Riera, V.; Miguel, D.; Kassel, S.; Rheingold, A. *Inorg. Chem.* **2002**, *41*, 4671. (b) Bergamo, M.; Beringhelli, T.; D'Alfonso, G.; Maggioni, D.; Mercandelli, P.; Sironi, A. *Inorg. Chim. Acta* **2003**, *350*, 475. (c) Fernandez, J. M.; Emerson, K.; Larsen, R. D.; Gladysz, J. A. *J. Chem. Soc., Chem. Commun*. **1988**, 37. (d) Dalton D. M.; Fernandez, J. M.; Emerson, K.; Larsen, R. D.; Arif, A .M.; Gladysz, J. A. *J. Am. Chem. Soc.* **1990**, *112*, 9198. (e) Davlieva, M. G.; Lindeman, S. V.; Neretin, I. S.; Kochi, J. K. *J. Org. Chem*. **2005**, *70*, 4013. (f) Weinert, C. S.; Fanwick, P. E.; Rothwell, I. P. *Organometallics* **2005**, *24*, 5759. (g) Sun, Y. M.; Piers, W. E.; Yap, G. P. A. *Organometallics* **1997**, *16*, 2509. (h) Chan, M. C. W.; Tam, K. H.; Zhu, N. Y.; Chiu, P.; Matsui, S. *Organometallics* **2006**, *25*, 785. (i) Cadierno, V.; Zablocka, M.; Donnadieu, B.; Igau, A.; Majoral. J. P.; Skowronska, A. *Chem.−Eur. J.* **2001**, *7*, 221. η^2-Acetophenone: see ref 39.

(43) Delbecq, F.; Sautet, P. *J. Am. Chem. Soc.* **1992**, *114*, 1446.

(44) Méndez, N. Q.; Seyler, J. W.; Arif, A. M. Gladysz, J. A. *J. Am. Chem. Soc.* **1993**, *115*, 2323.

(45) Burnett, M. G.; Morrison, R. J. *J. Chem. Soc. (A)* **1971**, 2325.

PPh_3 binding energy is especially sensitive when forming species such as **7b**, where there are three neighboring PPh_3 ligands. Under these circumstances the use of the BP86/UFF approach appears to be unreliable.

Conclusions

Density functional and hybrid density functional/Hartree−Fock calculations have been employed to model the β-H elimination reactions of *trans*-[Ir(XMe)(CO)$(PPh_3)_2$] species (X = O, CH_2). Activation barriers to β-H elimination are ca. 12 kca/mol higher for the alkoxide system, consistent with the greater stability of these species seen experimentally compared to their alkyl analogues. This difference results from the ability of alkoxide ligands to stabilize the unsaturated intermediate formed upon initial phosphine dissociation. A further isomerization barrier is then required before a β-agostic stabilized precursor to β-H transfer is accessed. For the acetophenone complex [Ir(η^2-O═C(Me)Ph)(CO)(PPh_3)], a low-energy pathway for exchange of the ketone face binding to the metal center has been located via an η^1-intermediate.

Acknowledgment. We thank Heriot-Watt University for the award of a James Watt Scholarship to P.V.

Supporting Information Available: Cartesian coordinates and energies of all computed species. Full ref 22. This material is available free of charge via the Internet at http://pubs.acs.org.

OM700276P

(46) Similar behavior has been seen when computing PPh_3 binding energies in [Pd(Me)(OMe)$(PPh_3)_2$] species. For the *cis* isomer a PPh_3 binding energy of 28.2 kcal/mol was computed at the BP86/UFF level for removal of PPh_3 *trans* to Me. This value fell by over half to 12.2 kcal/mol at both the BP86/HF and the BP86//BP86/HF levels. For the *trans* isomer BP86/UFF again gives the largest biding energy of 29.4 kcal/mol, and although this falls to 20.6 kcal/mol (BP86/HF) and 20.0 kcal/mol (BP86//BP86/HF), the difference is not as dramatic as in the *cis* isomer, where the two PPh_3 ligands are in close contact. Vadivelu, P. Ph.D. Thesis, Heriot-Watt University, 2007.